Journal of Anatomy

J. Anat. (2014) **224**, pp556–563 doi: 10.1111/joa.12163

Primordial germ cells in the dorsal mesentery of the chicken embryo demonstrate left–right asymmetry and polarized distribution of the EMA1 epitope

Gideon Hen,[1,2] Miriam Friedman-Einat[2] and Dalit Sela-Donenfeld[1]

[1]*Koret School of Veterinary Medicine, The Robert H. Smith Faculty of Agriculture, Food & Environment, The Hebrew University of Jerusalem, Rehovot, Israel*
[2]*ARO, Volcani Center, Bet-Dagan, Israel*

Abstract

Despite the importance of the chicken as a model system, our understanding of the development of chicken primordial germ cells (PGCs) is far from complete. Here we characterized the morphology of PGCs at different developmental stages, their migration pattern in the dorsal mesentery of the chicken embryo, and the distribution of the EMA1 epitope on PGCs. The spatial distribution of PGCs during their migration was characterized by immunofluorescence on whole-mounted chicken embryos and on paraffin sections, using EMA1 and chicken vasa homolog antibodies. While in the germinal crescent PGCs were rounded and only 25% of them were labeled by EMA1, often seen as a concentrated cluster on the cell surface, following extravasation and migration in the dorsal mesentery PGCs acquired an elongated morphology, and 90% exhibited EMA1 epitope, which was concentrated at the tip of the pseudopodia, at the contact sites between neighboring PGCs. Examination of PGC migration in the dorsal mesentery of Hamburger and Hamilton stage 20–22 embryos demonstrated a left–right asymmetry, as migration of cells toward the genital ridges was usually restricted to the right, rather than the left, side of the mesentery. Moreover, an examination of another group of cells that migrate through the dorsal mesentery, the enteric neural crest cells, revealed a similar preference for the right side of the mesentery, suggesting that the migratory pathway of PGCs is dictated by the mesentery itself. Our findings provide new insights into the migration pathway of PGCs in the dorsal mesentery, and suggest a link between EMA1, PGC migration and cell–cell interactions. These findings may contribute to a better understanding of the mechanism underlying migration of PGCs in avians.

Key words: chicken embryo; dorsal mesentery; EMA1; left–right asymmetry; neural crest cells; primordial germ cells.

Introduction

Chicken primordial germ cells (PGCs) and their migration route have become topics of great interest, not only because of their role as precursors of the germ cells, but also because they have become a compelling target for gene transfer toward the production of transgenic chicken lines (van de Lavoir et al. 2006; Macdonald et al. 2012). However, this process has only been partially characterized.

Correspondence
Dalit Sela-Donenfeld, Koret School of Veterinary Medicine, The Robert H. Smith Faculty of Agriculture, Food & Environment, The Hebrew University of Jerusalem, Rehovot 76100, Israel.
E: dalit.seladon@mail.huji.ac.il
and
Miriam Friedman-Einat, ARO, Volcani Center, P.O. Box 6, Bet-Dagan 50250, Israel. E: miri.einat@mail.huji.ac.il

Accepted for publication *4 January 2014*
Article published online *7 February 2014*

Similar to PGCs of other animals, chicken PGCs reach the gonads from an extragonadal site. Their journey begins in the epiblast (Eyal-Giladi et al. 1981), from which they ingress ventrally and migrate anteriorly during gastrulation toward the germinal crescent, where they accumulate until Hamburger and Hamilton (HH) stage 10 (Hamburger & Hamilton, 1951). There, unlike mammalian and amphibian PGCs, they utilize newly formed blood vessels through which they circulate and reach the embryonic body (Ando & Fujimoto, 1983). This process is manifested by a decreased number of PGCs in the germinal crescent beginning at HH stage 10, while in parallel the number of circulating PGCs rises (Nakamura et al. 2007).

As in mice, chicken PGCs were previously shown to migrate through the dorsal mesentery toward the genital ridge, yet they do not cross the gut epithelium, but rather reach the dorsal mesentery from the circulation at a site adjacent to the developing gonads (Ando & Fujimoto, 1983; Ukeshima et al. 1991). From this domain they were

suggested to actively migrate until they reach the genital ridge (Fujimoto et al. 1976), where they settle and differentiate into spermatogonia or oogonia (Kuwana & Rogulska, 1999). However, compared with other model animals, such as mice and zebrafish, fundamental issues regarding development of the chicken PGCs have not yet been resolved. These include their precise routes and modes of migration, intravasation and extravasation, and the factors guiding their migration.

Avian PGCs can be detected using specific markers, such as chicken vasa homolog (CVH; Tsunekawa et al. 2000) and Dead End genes (Aramaki et al. 2007). Alternatively, PGCs can be detected using markers that are not restricted only to PGCs, such as Nanog, PouV (Lavial et al. 2007), SSEA1 (Karagenc et al. 1996) and EMA1 (Hahnel & Eddy, 1986; Urven et al. 1988), or using the periodic acid-Schiff (PAS) staining (Meyer, 1960). EMA1 has been reported in the past to label mostly epiblast cells of chicken embryos, and to recognize only up to one-third of the PAS-positive cells at HH stage 20 (Urven et al. 1988). As specific PGC markers were not available at that time, as well as the utilization of double-labeling immunofluorescence methods, it remained unclear to what extent EMA1 marker is indeed presented by PGCs at different stages of development, how EMA1 epitope is distributed on PGC membranes, and what role may EMA1 play during PGC migration. Moreover, the precise morphology and migration pattern of the chicken PGCs at different stages and sites were not fully resolved.

Here we provide new data regarding migration pattern of PGCs in the chicken embryo, demonstrating the dynamic distribution of EMA1 on the cell surface of PGCs, their dramatic morphological changes at different sites and their asymmetric migration pattern in the dorsal mesentery. Together, these findings provide better understanding of the migration process of PGCs in avian.

Materials and methods

Embryos

Fertilized White Leghorn eggs were purchased from a local hatchery (Weisman, Sitryia, Israel). Eggs were incubated at 37.8 °C in a humidified incubator for the indicated periods. Embryos were collected and fixed in 4% paraformaldehyde (PFA) in phosphate-buffered saline (PBS) at 4 °C overnight, and staged according to HH (Hamburger & Hamilton, 1951).

Immunofluorescence

Immunofluorescence of paraffin sections was performed as described previously (Hen et al. 2012). For whole-mount detection of PGCs in the dorsal mesentery and genital ridge, midline tissues, including mesonephros, dorsal mesentery and gut, were isolated and stained in one piece. Prior to detection, tissues were treated with modified Dent solution [methanol : dimethylsulfoxide (DMSO) : H_2O_2 at a ratio of 2 : 1 : 3, v/v] at room temperature overnight, washed in methanol and gradually rehydrated in PBS. Rabbit anti-CVH antibody (diluted 1 : 2400) was kindly provided by Prof. T. Noce (Tsunekawa et al. 2000). Mouse anti-EMA1 and fibronectin antibodies were obtained as supernatants from Developmental Studies Hybridoma Bank (Iowa City, IA, USA). Mouse anti-HNK-1 (1 : 500) was purchased from BD Biosciences. Rabbit anti-phospho Histone-H3 (1 : 200) was obtained from Santa Cruz (Almog Diagnostic, Israel). Secondary antibodies included Alexa Fluor 488 and Alexa Fluor 594 goat anti-rabbit or goat anti-mouse (1 : 500 each; Invitrogen, Rhenium, Israel). Whole-mount rhodamine-phalloidin staining (50 μg mL^{-1}) was performed by 1-h incubation at room temperature, followed by three washes with PBS-T (0.05% Tween-20). Nuclei were counterstained with 4′,6-diamidino-2-phenylindole (DAPI; Sigma-Aldrich, Israel), and samples were mounted on slides and covered using Fluoro-Gel (EMS, Bar-Naor, Israel).

Embryo sex determination

Thirty embryos were collected and staged according to HH (Hamburger & Hamilton, 1951). The head was dissected and used for individual extraction of genomic DNA. The dorsal mesentery was isolated with the mesonephros and the gut, and fixed in 4% PFA. Following fixation, tissues were subjected individually to immunofluorescence as described before, in order to examine asymmetry in migration through the dorsal mesentery. Sex determination of embryos was done by polymerase chain reaction (PCR) using 100 ng of genomic DNA, according to Fridolfsson & Ellegren (1999), with the 2550F/2718R primers, using the Green Master Mix (Promega). Products were resolved on a 1.7% agarose gel, and sex was determined by product size: 600 bp for male, or 600 bp and 450 bp for female.

Microscopy

Images of whole-mounted specimens were taken using the Olympus SZX16 epifluorescent stereomicroscope, equipped with an Olympus DP72 camera. Confocal images were obtained using an Olympus IX81 inverted laser-scanning microscope with Fluoview-500 software. Digital images of paraffin sections were taken using a Nikon Eclipse e400 upright microscope, equipped with an Olympus DP72 camera and Olympus DP Controller software.

Statistical analysis

Data are presented as the mean $\pm$ standard error recorded from four different samples at each developmental stage. Data for the ratio of $EMA1^+$ PGCs were analyzed by one-way ANOVA. Data for left–right asymmetry in PGC migration in the dorsal mesentery were analyzed using the Student's *t*-test. Differences were regarded as significant at $P < 0.05$. Data were analyzed using JMP (SAS Institute).

Results

Dynamic distribution of EMA1 on cell surface of PGCs

The chicken PGCs have a unique route of migration, including embryonic and extraembryonic migration, as well as a

circulatory phase. At present, CVH serves as a powerful specific marker to detect migrating PGCs (Tsunekawa et al. 2000), while several past studies used EMA1 to detect PGCs (Hahnel & Eddy, 1986; Urven et al. 1988). Because EMA1 was also detected in cells other than PGCs, and was reported to be present only in a subset of PGCs (Urven et al. 1988), we aimed here to unravel the migration dynamics of PGCs in relation to EMA1 labeling by studying the co-labeling of CVH and EMA1 in PGCs, and the precise distribution of EMA1 on their surface. Therefore, we characterized the distribution of EMA1 epitope on the PGC cell surface by whole-mount immunostaining of chicken embryos, followed by confocal imaging. Examination of the germinal crescent of HH stages 8 and 14 (Fig. 1A and E, respectively) revealed variation in EMA1 labeling, manifested by PGCs that exhibit $EMA1^{+}$ next to $EMA1^{-}$ PGCs (Fig. 1C,D,G,H), whereas all PGCs were similarly stained with CVH (Fig. 1B,F). The percentages of PGCs co-labeled with CVH and EMA1 in the germinal crescent at these stages were $24.2 \pm 2.3\%$ and $32.8 \pm 5.2\%$, respectively ($n = 4$ embryos for each stage, with over 40 cells analyzed for each embryo). Moreover, although cells were round at these stages, EMA1 staining exhibited a cluster of intensified staining (Fig. 1C, G, arrowheads, and Supporting Information Movie S1). At that time, and in addition to PGCs, ectodermal cells were also found to present the EMA1 epitope, which was located at cell boundaries (Fig. 1I,J), in contrast to its restricted accumulation in PGCs.

Subsequent assessment of CVH and EMA1 labeling of PGCs at HH stages 20–22, during their migration through the dorsal mesentery toward the genital ridge, revealed that they had lost their round morphology and acquired a more elongated shape. At these stages, cells were polarized and exhibited distinct pseudopodia (Fig. 2D), as also evident

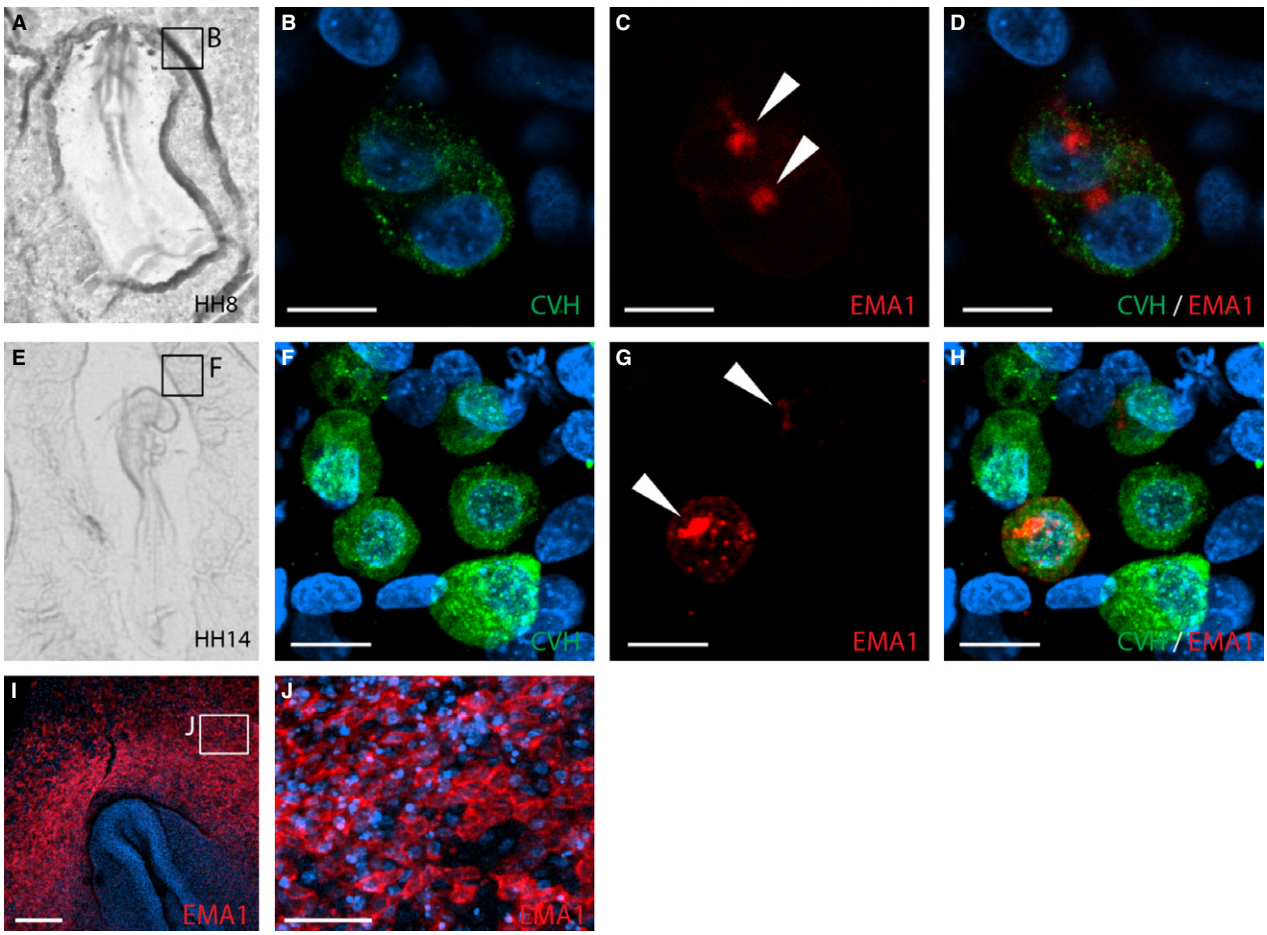

Fig. 1 EMA1 and chicken vasa homolog (CVH) labeling in PGCs during migration toward the germinal crescent. (A, E) Bright-field images of embryos used for analysis. (B–D, F–H) Confocal analysis of PGCs observed in fluorescent whole-mount preparations of the boxed areas marked in (A) and (E), respectively, using EMA1 (red) and CVH (green) antibodies. Nuclei were counterstained with DAPI (blue). CVH is evenly distributed in all PGCs (B, F) while EMA1 is not present on all cells, but rather aggregates unequally in PGCs (C, G, arrowheads). (D, H) Merged images of (B, C) and (F, G), respectively. (I) Whole-mount image of Hamburger and Hamilton (HH) stage 8 embryo, demonstrating ectodermal staining of EMA1. (J) High magnification of cells in (I), demonstrating EMA1 staining along boundaries between adjacent cells. Scale bar: 10 μm (B–D, F–H); 200 μm (I); 50 μm (J).

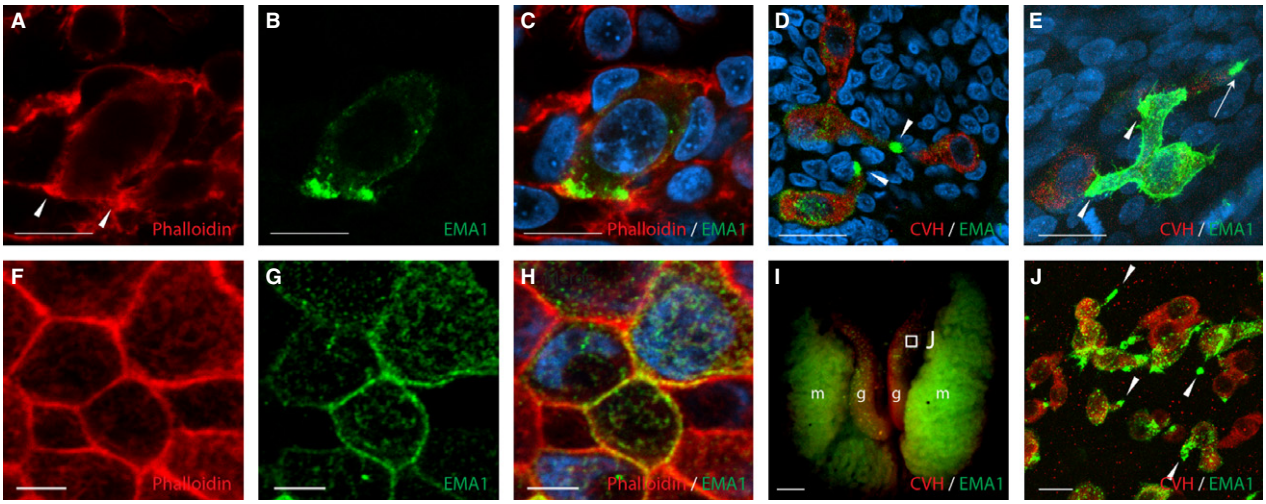

Fig. 2 EMA1 epitope on PGCs is concentrated at sites of cell–cell contact. Whole-mount immunofluorescence of HH stage 20 embryos, demonstrating phalloidin staining of actin fibers (A) and EMA1 staining (B), co-localized to the elongated edges of a PGC, the contact sites with neighboring cells (C) or with other PGCs (D, E, arrowheads). Polarized EMA1 staining is also demonstrated for PGCs in the gonads of E7 embryos (I, J). (J) is an enlargement of the boxed area in (I). Epithelial cells examined at similar stages show non-polarized actin staining (F) and uniform EMA1 labeling at the cell surface (G, H). CVH, chicken vasa homolog; g, gonad; m, mesonephros. Scale bar: 10 μm (A–E); 5 μm (F–H); 1 mm (I); 50 μm (J).

by condensed actin labeling at the cell tip using phalloidin (Fig. 2A, arrowheads). Noticeably, while CVH was uniformly expressed at PGCs cytoplasm, EMA1 staining was unequally distributed on the cell surface, concentrating at the tip of the cells, at sites of cell–cell interaction (Fig. 2B,D). In fact, the tip of the pseudopodia remained the site of a more intensified staining among all PGCs with elongated morphology (Fig. 2D, arrowheads), and although some PGCs were labeled with EMA1 more intensely than others, EMA1 labeling was constantly strongest at sites where contact with neighboring PGCs was established (Fig. 2E, arrowheads). In addition, some PGCs exhibited an ability to simultaneously interact with more than a single PGC (Fig. 2E). At that stage, and in contrast to migrating PGCs, epithelial cells in the embryo, which exhibited a cubical morphology, were characterized by uniform actin staining (Fig. 2F), along with even distribution of EMA1 on the cell membrane (Fig. 2G, H). The polarized distribution of EMA1 in PGCs could also be detected after PGCs had reached the gonads (Fig. 2I,J). Here again, the unequal distribution of EMA1 epitope localized to the pseudopodia (Fig. 2J, arrowheads) was prominent on the background of CVH, which stained all PGCs equally. In contrast to earlier stages, the percentage of EMA1-labeled PGCs in the dorsal mesentery was significantly higher, as the majority of PGCs were co-labeled with EMA1 and CVH (89 $\pm$ 5.7%, $n = 4$ embryos, $P < 0.0001$).

Altogether, these data demonstrate the dynamic rounded-to-elongated morphology of PGCs during their migration from the germinal crescent to the gonads, accompanied by polarization of EMA1 epitope, concentrating at the sites of cell–cell interaction during PGCs migration in the dorsal mesentery.

Left–right asymmetry in migration of PGCs in the dorsal mesentery

Distribution of PGCs in the gonads of chicken embryos was described before, including important findings regarding the mechanism regulating left–right asymmetry between the gonads (Ishimaru et al. 2008; Rodriguez-Leon et al. 2008). Moreover, left–right asymmetry in the numbers of PGCs was previously found in the intermediate mesoderm at earlier stages (Nakamura et al. 2007). However, the migratory behavior of chicken PGCs in the dorsal mesentery, the tissue through which the PGCs migrate toward the genital ridge after extravasation, has not been characterized yet. To address this issue, chicken embryos at HH stages 20–22 were subjected to whole-mount immunofluorescence using CVH and EMA1 antibodies. This analysis revealed a clear left–right asymmetry in migration of PGCs along the dorsal mesentery, in a dorsolateral direction toward the genital ridges, manifested by restricted localization of PGCs to the right side of the mesentery. Following removal of the gut, the ventral view of the mesentery (Fig. 3A; between two dashed lines) showed relatively medial localization of PGCs migrating to the right genital ridge, compared with PGCs migrating left, which seemed lateral to the mesentery, with some detected as clusters (Fig. 3A, arrowheads) or chains of cells (Fig. 3A, arrow, B). The left–right asymmetry observation was clearly detected in 15 out of 30 embryos at HH stages 20–22 examined, with an average of 30 $\pm$ 5 vs. 6 $\pm$ 1.3 cells on the right and left sides of the mesentery, respectively ($P < 0.01$, $n = 4$ embryos), while in other embryos the number of PGCs was similar between left and right sides of the mesentery. These results were in agreement with

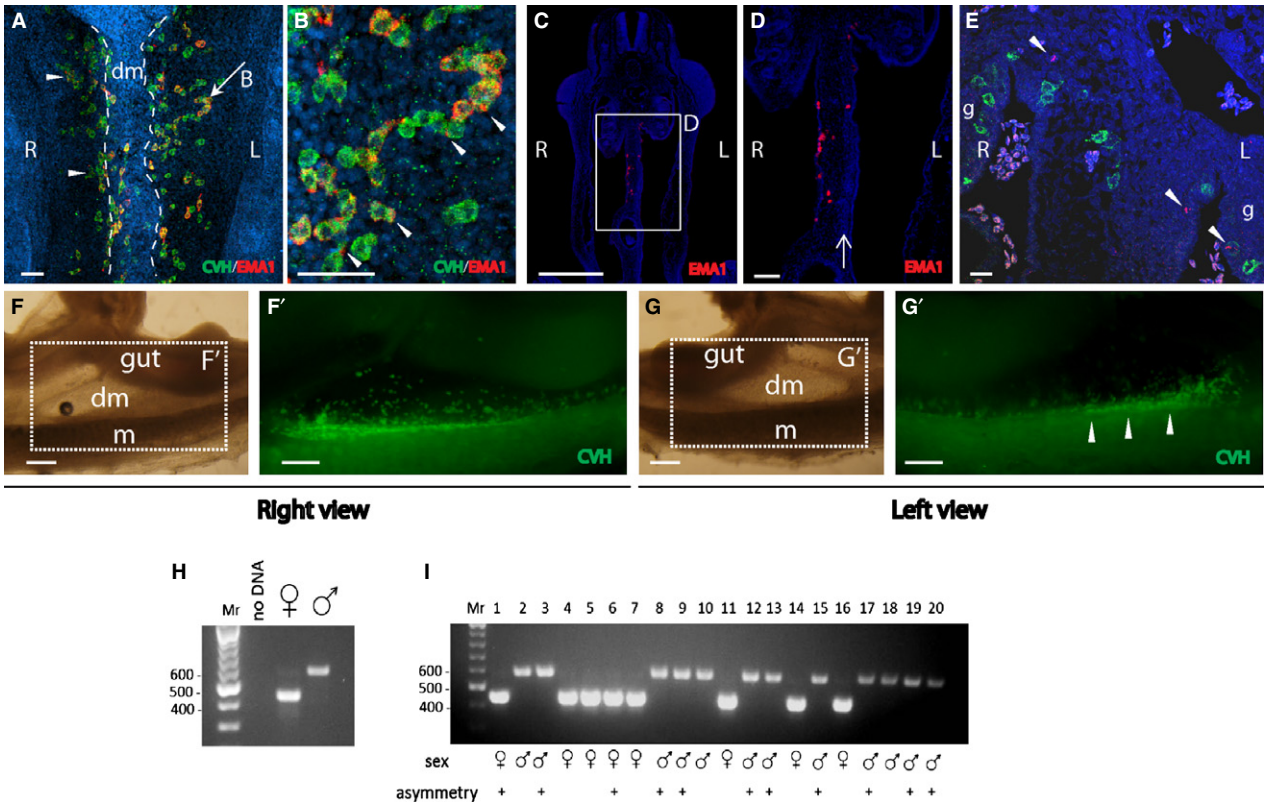

Fig. 3 Left–right asymmetry in migration of PGCs through the dorsal mesentery. Immunofluorescence on whole-mount (A–B, F′, G′) and paraffin sections (C–E) of HH stages 20–22 embryos, using chicken vasa homolog (CVH) and EMA1 antibodies. (A) In HH stage 20 embryos, PGCs are present on the right but not left side of the mesentery. The PGCs on the left side are observed migrating toward the genital ridge. Cells were detected as clusters (arrowheads) or chains (arrow). (B) Field magnification of PGC-chain indicated by an arrow in (A). Examples for polarized EMA1 staining are indicated by arrowheads. (C, D) Coronal section of HH stage 20 embryo demonstrating PGCs on the right side of the mesentery. Area of condensed mesodermal cells on the left side of the mesentery is indicated by an arrow. (E) Co-labeling of EMA1 and pHistone-H3 demonstrating the asymmetrical distribution of PGCs vs. equal distribution of pHistone-H3 (arrowheads). (F–G′) Right (F–F′) and left (G–G′) views of the mesentery of a HH stage 22 embryo immunostained for CVH (F′,G′). PGCs can be seen on the right side of the mesentery (F′). A left view of the same area reveals only a faded signal of PGCs from the right side (G′), while most PGCs have reached the genital ridge (G′, arrowheads). (H) Sex determination using PCR. Negative control (no DNA) and positive controls (female and male) are shown. (I) PCR results of 20 representative DNA samples, isolated from chicken embryos. The sex of each embryo and the presence of asymmetry in migration are indicated. dm, dorsal mesentery; g, gonad; L, left; m, mesonephros; R, right. Scale bar: 50 μm (A, B); 80 μm (C, D); 1 mm (E, E′, F, F′).

coronal sections of embryos at these stages, demonstrating the presence of PGCs on the right side, but not on the left side of the mesentery (Fig. 3C,D), which is typically characterized by more condensed cells compared with the right half of the dorsal mesentery (Fig. 3D, arrow; Davis et al. 2008). Noticeably, distribution of other general markers, such as pHistone-H3 (Fig. 3E) was symmetrical in the embryo. Lateral views of the dorsal mesentery of HH stage 22 embryos (Fig. 3F,G) showed that while PGCs on the right side of the mesentery were easily detected (Fig. 3F′), PGCs on the left side were detected only in the genital ridge (Fig. 3G′, arrowheads), further supporting the notion of a left–right asymmetry in PGC migration in the dorsal mesentery, manifested by restriction of PGCs to the right side of the mesentery. Notably, not a single opposite case was found.

Since the right ovary of the female chicken embryo undergoes regression during development, and because asymmetry in colonization of PGCs in the gonads was shown to correlate with the sex of the embryo (Clawson & Domm, 1963; Ono et al. 1996), we examined whether the left–right asymmetry in PGC migration in the dorsal mesentery correlates with the sex of the embryo. For that purpose, genomic DNA was isolated individually from the head of each embryo prior to fixation and immunofluorescence. This DNA was used for sex determination by PCR, using primers for the chromo-helicase DNA-binding gene (Fig. 3H). This analysis revealed that at the examined stages, asymmetry in migration through the dorsal mesentery was detected in both male and female embryos (Fig. 3I), therefore it cannot be attributed to the sex of the embryo. Altogether, the results demonstrated a first documentation for a left–right asymmetry in the migration of PGCs in the dorsal mesentery toward the genital ridge, shared by both male and female embryos.

Because this observation does not correlate with the sex of the embryo, it may be attributed to intrinsic asymmetric properties of the dorsal mesentery tissue. In such a scenario, asymmetry in the dorsal mesentery tissue may influence the migration route of additional cells passing through the dorsal mesentery. To test this hypothesis we examined migration of the enteric neural crest cells (NCCs), known to cross the dorsal mesentery before colonizing the gut. Staining of paraffin sections using HNK-1 antibody, a marker for migratory NCCs, revealed asymmetric migration of NCCs, restricted to the right side of the dorsal mesentery (Fig. 4A, B). Double-labeling using HNK-1 and EMA1 antibodies demonstrated the asymmetric migration route shared by both PGCs and NCCs (Fig. 4C). Interestingly, staining of the ECM marker fibronectin, which is known to label the migration route of NCCs (Perris & Perissinotto, 2000), was also restricted to the right side of the mesentery, yet did not overlap with HNK-1 signal (Fig. 4D), therefore supporting our suggestion for asymmetry in NCC migration. This was in contrast to the uniform expression of HNK-1 and fibronectin at sites other than the dorsal mesentery such as the aorta and gut (Fig. 4E, asterisk, and data not shown). Co-staining of embryos with HNK-1 and pHistone-H3 demonstrates the localized vs. symmetrical expression of each marker, respectively, further excluding the possibility of apparent asymmetry in the dorsal mesentery due to technical reasons. Altogether, the results suggest that asymmetric properties of the dorsal mesentery may dictate asymmetrical position of migrating PGCs and NCCs through the mesentery.

Discussion

This study was aimed at gaining new insights into the migratory behavior of PGCs in avian embryos. We utilized the PGC markers EMA1 and CVH to examine the migration, cell–cell interactions and distribution of EMA1 on the surface of PGCs, and found that EMA1 staining on the cell surface varies among PGCs during embryonic development. At early stages, when PGCs display a round morphology, EMA1 epitope is present on some, but not all, PGCs, where it usually concentrates as a cluster on the cell surface. Yet, in contrast to a previous report (Urven et al. 1988), we showed that at subsequent stages of development, in the dorsal mesentery and later in the gonads, PGCs become elongated and EMA1 labels almost the entire PGC population. At these sites, EMA1 epitope is concentrated at the tip of the PGC pseudopodia. These morphological changes are accompanied by actin polarization, as evident using phalloidin staining. Noticeably, the leading edge of many other types of migrating cells is involved in sensing chemoattractants in their environment (Swaney et al. 2010) and, moreover, PGCs are considered to actively migrate toward a chemoattractant gradient from the genital ridge (Stebler et al. 2004). Hence, it is possible that the increased percentage of EMA1-labeled PGCs in the dorsal mesentery, together with EMA1 accumulation at the cell's tip, allow it to play a role in the interaction of migrating PGCs with the environment during their active migration. The observation of enhanced EMA1 staining at sites of physical contact between neighboring PGCs further supports a putative function of this glycoprotein in the interaction between actively migrating PGCs in the chicken embryo, which awaits to be confirmed.

Previously, left–right asymmetry in the numbers of PGCs in the intermediate mesoderm was described at earlier developmental stages (Nakamura et al. 2007). Our data showed for the first time a difference in the spatial distribution of PGCs in the dorsal mesentery, and in more advanced embryos. Notably, a previous study found no sign of asymmetry in PGC migration through the dorsal mesentery (Davis et al. 2008). However, this was addressed by transverse sections of the dorsal mesentery, rather than by whole-mount immunostaining or coronal sections, and we believe that the former sectioning strategy prevented this observation. The fact that half of the examined embryos

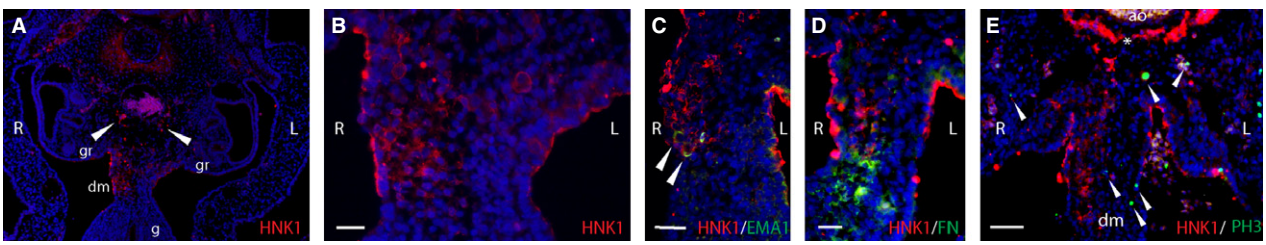

Fig. 4 Asymmetry of HNK-1-labeling in paraffin sections of the dorsal mesentery. (A) A section of HH stage 20 embryo, immunostained using HNK-1 antibody. Nuclei were stained with DAPI (blue). Arrowheads indicate streams of neural crest cells migrating ventrally toward the mesentery and the gut. (B) A magnified view of the dorsal mesentery seen in (A) shows asymmetrical HNK-1 staining. Note the difference in nuclei density between left and right sides of the mesentery. (C) Co-labeling of HNK-1 and EMA1 (arrowheads) in the right side of the dorsal mesentery. (D) HNK-1 and fibronectin staining share the right side of the dorsal mesentery, yet do not overlap. (E) Embryo section stained with pHistone-H3 (arrowheads) and HNK-1. Note the expression of HNK-1, restricted to the right side of the mesentery compared with its uniform expression in the aorta (asterisk). pHistone-H3 is distributed at different embryonic sites. ao, aorta; dm, dorsal mesentery; g, gut; gr, genital ridge; L, left; R, right. Scale bar: 80 μm (A); 40 μm (D); 20 μm (B, C, E).

exhibited this migration asymmetry could be attributed to variation in development of the mesentery among embryos or, alternatively, may suggest a sex-linked phenotype, as left–right asymmetry is a hallmark of the avian female reproduction system, characterized by regression of the right ovary. In an attempt to examine a link between the asymmetry and the sex of the embryo, we determined the sex of 30 embryos prior to staining of PGCs in the dorsal mesentery, yet we could not find such a correlation. Hence, another possible mechanism responsible for this observation could be the asymmetry in cellular and genetic profiles described in the dorsal mesentery (Davis et al. 2008), manifested by the asymmetry in cell density in the mesentery, as shown here and by Davis et al. (2008). Paraffin sections stained using HNK-1 revealed that in addition to PGCs, the NCCs also cross the dorsal mesentery in an asymmetric fashion, suggesting that the cellular and/or extracellular properties of the dorsal mesentery dictate the route of migration of other cell types, additionally to PGCs. In this regard, a previous report suggested that human PGCs preferentially migrate along nerve fibers in the dorsal mesentery (Mollgard et al. 2010), thereby supporting our suggestion for shared and overlapping asymmetric migration of PGCs and NCCs in the dorsal mesentery of the chicken embryo, and raising an interesting question regarding a possible role of PGCs in development of the peripheral nervous system and vice versa. Altogether, these findings provide new insight into the migratory pathway of PGCs in the chicken, and suggest an interaction between development of the dorsal mesentery and the spatio-temporal distribution of PGCs. Future studies will be required in order to decipher the mechanism that induces migration asymmetry in the dorsal mesentery, and the interplay between the mesentery and migrating PGCs. These studies should also examine the link between this observation and development of the reproduction system of the chicken embryo.

Acknowledgements

The authors are grateful to Prof. T. Noce, Japan, for kindly providing us with the CVH antibody. The authors also thank Eduard Belausov, The Institute of Plant Sciences, ARO, for the highly professional help with the confocal imaging.

References

Ando Y, Fujimoto T (1983) Ultrastructural evidence that chick primordial germ cells leave the blood-vascular system prior to migrating to the gonadal anlagen. *Dev Growth Differ* **25**, 345–352.

Aramaki S, Sato F, Kato T, et al. (2007) Molecular cloning and expression of dead end homologue in chicken primordial germ cells. *Cell Tissue Res* **330**, 45–52.

Clawson RC, Domm LV (1963) Developmental changes in glycogen content of primordial germ cells in chick embryo. *Proc Soc Exp Biol Med* **112**, 533–537.

Davis NM, Kurpios NA, Sun X, et al. (2008) The chirality of gut rotation derives from left–right asymmetric changes in the architecture of the dorsal mesentery. *Dev Cell* **15**, 134–145.

Eyal-Giladi H, Ginsburg M, Farbarov A (1981) Avian primordial germ cells are of epiblastic origin. *J Embryol Exp Morphol* **65**, 139–147.

Fridolfsson AK, Ellegren H (1999) A simple and universal method for molecular sexing of non-ratite birds. *J Avian Biol* **30**, 116–121.

Fujimoto T, Ukeshima A, Kiyofuji R (1976) The origin, migration and morphology of the primordial germ cells in the chick embryo. *Anat Rec* **185**, 139–145.

Hahnel AC, Eddy EM (1986) Cell surface markers of mouse primordial germ cells defined by two monoclonal antibodies. *Gamete Res* **15**, 25–34.

Hamburger V, Hamilton HL (1951) A series of normal stages in the development of the chick embryo. *Dev Dyn* **195**, 231–272.

Hen G, Yosefi S, Shinder D, et al. (2012) Gene transfer to chicks using lentiviral vectors administered via the embryonic chorioallantoic membrane. *PLoS ONE* **7**, e36531.

Ishimaru Y, Komatsu T, Kasahara M, et al. (2008) Mechanism of asymmetric ovarian development in chick embryos. *Development* **135**, 677–685.

Karagenc L, Cinnamon Y, Ginsburg M, et al. (1996) Origin of primordial germ cells in the prestreak chick embryo. *Dev Genet* **19**, 290–301.

Kuwana T, Rogulska T (1999) Migratory mechanisms of chick primordial germ cells toward gonadal anlage. *Cell Mol Biol (Noisy-le-grand)* **45**, 725–736.

Lavial F, Acloque H, Bertocchini F, et al. (2007) The Oct4 homologue PouV and Nanog regulate pluripotency in chicken embryonic stem cells. *Development* **134**, 3549–3563.

van de Lavoir MC, Diamond JH, Leighton PA, et al. (2006) Germline transmission of genetically modified primordial germ cells. *Nature* **441**, 766–769.

Macdonald J, Taylor L, Sherman A, et al. (2012) Efficient genetic modification and germ-line transmission of primordial germ cells using piggyBac and Tol2 transposons. *Proc Natl Acad Sci USA* **109**, E1466–E1472.

Meyer DB (1960) Application of the periodic acid-schiff technique to whole chick embryos. *Biotech Histochem* **35**, 83–89.

Mollgard K, Jespersen A, Lutterodt MC, et al. (2010) Human primordial germ cells migrate along nerve fibers and Schwann cells from the dorsal hind gut mesentery to the gonadal ridge. *Mol Hum Reprod* **16**, 621–631.

Nakamura Y, Yamamoto Y, Usui F, et al. (2007) Migration and proliferation of primordial germ cells in the early chicken embryo. *Poult Sci* **86**, 2182–2193.

Ono T, Yokoi R, Aoyama H (1996) Transfer of male or female primordial germ cells of quail into chick embryonic gonads. *Exp Anim* **45**, 347–352.

Perris R, Perissinotto D (2000) Role of the extracellular matrix during neural crest cell migration. *Mech Dev* **95**, 3–21.

Rodriguez-Leon J, Rodriguez Esteban C, Marti M, et al. (2008) Pitx2 regulates gonad morphogenesis. *Proc Natl Acad Sci USA* **105**, 11 242–11 247.

Stebler J, Spieler D, Slanchev K, et al. (2004) Primordial germ cell migration in the chick and mouse embryo: the role of the chemokine SDF-1/CXCL12. *Dev Biol* **272**, 351–361.

Swaney KF, Huang CH, Devreotes PN (2010) Eukaryotic chemotaxis: a network of signaling pathways controls motility, directional sensing, and polarity. *Annu Rev Biophys* **39**, 265–289.

Tsunekawa N, Naito M, Sakai Y, et al. (2000) Isolation of chicken vasa homolog gene and tracing the origin of primordial germ cells. *Development* **127**, 2741–2750.

Ukeshima A, Yoshinaga K, Fujimoto T (1991) Scanning and transmission electron microscopic observations of chick primordial germ cells with special reference to the extravasation in their migration course. *J Electron Microsc (Tokyo)* **40**, 124–128.

Urven LE, Erickson CA, Abbott UK, et al. (1988) Analysis of germ line development in the chick embryo using an anti-mouse EC cell antibody. *Development* **103**, 299–304.

Supporting Information

Additional Supporting Information may be found in the online version of this article:

Movie S1. Three-dimensional confocal illustration of EMA1 labeling in PGCs. HH stage 14 chicken embryo was subjected to whole-mount immunofluorescence using EMA1 and CVH antibodies. CVH is evenly distributed in all PGCs while EMA1 is not present on all cells, and aggregates unequally on some of the PGCs.